

# Methane conversion to C<sub>2</sub> hydrocarbons and hydrogen in atmospheric non-thermal plasmas generated by different electric discharge techniques

Xiao-Song Li<sup>a</sup>, Ai-Min Zhu<sup>a,b,\*</sup>, Kang-Jun Wang<sup>a</sup>, Yong Xu<sup>a,b</sup>, Zhi-Min Song<sup>a</sup>

<sup>a</sup>Laboratory of Plasma Physical Chemistry, Dalian University of Technology, Dalian 116024, China

<sup>b</sup>State Key Laboratory for Material Modification by Laser, Ion and Electron Beams, Dalian University of Technology, Dalian 116024, China

## Abstract

Methane conversion to C<sub>2</sub> hydrocarbons and hydrogen has been investigated in a needle-to-plate reactor by pulsed streamer and pulsed spark discharges and in a wire-to-cylinder dielectric barrier discharge (DBD) reactor by pulsed DC DBD and AC DBD at atmospheric pressure and ambient temperature. In the former two electric discharge processes, acetylene is the dominating C<sub>2</sub> products. Pulsed spark discharges gives the highest acetylene yield (54%) and H<sub>2</sub> yield (51%) with 69% of methane conversion in a pure methane system and at 10 SCCM of flow rate and 12 W of discharge power. In the two DBD processes, ethane is the major C<sub>2</sub> products and pulsed DC DBD provides the highest ethane yield. Of the four electric discharge techniques, ethylene yield is less than 2%. Energy costs for methane conversion, acetylene or ethane (for DBD processes) formation, and H<sub>2</sub> formation increase with methane conversion percentage, and were found to be: in pulsed spark discharges (methane conversion 18–69%), 14–25, 35–65 and 10–17 eV/molecule; in pulsed streamer discharges (methane conversion 19–41%), 17–21, 38–59, and 12–19 eV/molecule; in pulsed DBD (methane conversion 6–13%), 38–57, 137–227 and 47–75 eV/molecule; in AC DBD (methane conversion 5–8%), 116–175, 446–637, and 151–205 eV/molecule, respectively. The immersion of the  $\gamma$ -Al<sub>2</sub>O<sub>3</sub> pellets in the pulsed streamer discharges, or in the pulsed DC DBD, or in the AC DBD has a positive effect on increasing methane conversion and C<sub>2</sub> yield.

© 2004 Elsevier B.V. All rights reserved.

**Keywords:** Methane conversion; Pulsed streamer discharges; Pulsed spark discharges; DBD

## 1. Introduction

The investigations of methane coupling to C<sub>2</sub> hydrocarbons in non-thermal plasmas have been made worldwide by corona discharges, or spark discharges, or dielectric barrier discharges (DBD) at atmospheric pressure and ambient temperature [1–12]. Liu et al. [1] studied methane conversion by direct current (DC) corona discharges. They found that ethane was the dominating product by corona discharges alone, and methane conversion to acetylene increased remarkably by corona discharges with NaY catalyst. Later studies show that methane can be converted to acetylene with high selectivity by pulsed corona or spark discharges without the use of catalyst. Kado et al. [2] investigated methane conversion in a needle-to-needle

reactor by pulsed DC discharges. Methane conversion was reported to be about 52% with 95% of acetylene selectivity at about 52 W of supplied power and 10 ml/min of methane flow rate. We have reported earlier that 44.6% of methane conversion and 67.5% of acetylene selectivity could be obtained by pulsed corona discharges at 1788 kJ/mol of energy density [3].

Recently, attentions have been paid to the effect of discharge techniques on methane conversion and product selectivity. For example, Yao et al. [4] investigated the influence of rising time of pulse voltage on methane conversion. Their study showed that rising time had remarkable effects on the selectivities of acetylene and ethane when the frequency of pulse was less than 2000 pulses per second (PPS). It was believed that methane conversion using this kind of pulsed plasma was going through pulsed spark discharge enhanced thermal pyrolysis [5]. Besides rising time, specific energy input per pulse also

\* Corresponding author.

E-mail address: [amzhu@dlut.edu.cn](mailto:amzhu@dlut.edu.cn) (A.-M. Zhu).

has an important effect on methane conversion and product selectivity. Yang [6] examined methane conversion in different discharges, such as glow discharges, DBD, corona discharges. It was found that product selectivity depended on discharge conditions and high acetylene selectivity was achieved at high specific energy input. Recently, Kado et al. [7] investigated methane conversion by corona or spark discharges and DBD, and emission spectroscopy was also used to study reaction mechanism. The results show that energy efficiency in spark discharges was much higher than that in DBD or corona discharges. In spark discharges, methane was mainly dissociated into atomic carbon and hydrogen by electron impact, and the high selectivity of acetylene was not caused by thermal pyrolysis.

In DBD process, both AC voltage [6–9], and pulsed DC voltage were used for methane conversion. Jeong et al. [10] studied methane conversion by pulsed DC DBD. The maximum methane conversion was about 25% and ethane selectivity was about 70–80%. The effect of alumina pellets filled in gas gap was also discussed and it was found that they played a role in enhancing ethane selectivity.

Previously, we have investigated methane coupling in a wire-to-cylinder reactor using fast-rising narrow pulsed voltage [3,11]. In this paper, in a needle-to-plate reactor, pulsed streamer discharges using fast-rising narrow pulsed voltage and pulsed spark discharge for methane coupling were studied. Then, methane conversions in pulsed streamer discharges, pulsed spark discharges, pulsed DC DBD and AC DBD were compared. The effects of the immersion of the  $\gamma$ - $\text{Al}_2\text{O}_3$  pellets in the plasmas generated by the four different discharge techniques were also examined.

## 2. Experimental

Four kinds of electric discharges, pulsed streamer discharges, pulsed spark discharges, pulsed DC DBD and AC DBD were investigated in this study. Electric circuit diagrams of the four kinds of electric discharges are shown in Fig. 1. As shown in Fig. 1(a), the fast-rising narrow pulse needed for producing pulsed streamer discharges in a reactor with needle-to-plate electrodes was provided by a circuit, consisting of energy-stored capacitor  $C_1$  (2200 pF), pulse forming capacitor  $C_2$  (255 or 550 pF) and rotary spark gap (RSG). A tungsten needle (1 mm diameter) was used as the high-voltage electrode and an iron plate (9 mm diameter) was used as the ground electrode. The distance from needle-to-plate was 10 mm in pulsed streamer discharges. A circuit consisting of a resistor  $R$  (5100  $\Omega$ ) and a capacitor  $C_1$  (2200 pF), as shown in Fig. 1(b), was used to generate pulsed spark discharges in a reactor with needle-to-plate electrodes. The distance from the needle to the plate is 6 mm. The frequency of discharge varies with voltage,  $RC$  time constant, and the character of reactor.

The reactor for DBD consists of an outer quartz tube (i.d. 10 mm, o.d. 13 mm) and a 2 mm-diameter stainless steel

wire placed along the axis of the outer tube as the high-voltage electrode. Aluminum foil wound on the outside surface of the outer tube was used as the ground electrode. The radial gas gap was 4 mm and the discharge volume was about 14 cm<sup>3</sup>. As to pulsed DC DBD, the pulsed voltage was also generated by RSG (electric circuit layout shown in Fig. 1(c)). The AC DBD process was provided with high voltage of bipolar sine wave at AC frequency of 50 Hz (Fig. 1(d)).

The voltage and current waveforms were measured by an oscilloscope (LeCroy LT-322) through the voltage probe (Tektronix P6015A or Iwatsu HV-P60) and the current probe (Tektronix A6303). The typical voltage waveforms of the four kinds of electric discharges were shown in Fig. 2. For all the four discharges, the total input power,  $P_t$ , was measured using a wattmeter in the primary side of the transformer. The discharge power of the reactors,  $P_{\text{discharge}}$ , in each discharge process was obtained by the methods mentioned below.

For the case of pulsed streamer discharges, it was assumed that the energy stored in the pulse forming capacitor approximately equals to the energy released into the reactor. So the discharge power,  $P_{\text{discharge}}$ , was calculated using the following equation:

$$P_{\text{discharge}} = 0.5fC_2U^2$$

where  $f$  is the pulse frequency (PPS),  $C_2$  the capacitance of the pulse forming capacitor, and  $U$  the voltage onto the pulse forming capacitor, which was measured using a high resistance of 1000 M $\Omega$  probe (HV-P60, IWATSU).

For the case of pulsed spark discharges, the discharge power was obtained by averaging the product of the voltage and current waveforms.

For pulsed DBD, owing to serious electromagnetic noises, the discharge power was determined by the method described in reference [13].

For the case of AC DBD, the discharge power was measured via the area of voltage–charge Lissajous figures [14].

All the experiments were performed under atmospheric pressure and at ambient temperature. The flow rate of methane (purity 99.9%) was adjusted and controlled by mass flow meters. The effluent gas from the reactor was analyzed with two online gas chromatographs (Agilent 1790F and 1790T) placed in a shielding room to avoid electromagnetic noises. One gas chromatograph was equipped with a flame ionization detector (FID) and a 3 m Porapak P column; the other gas chromatograph was equipped with a thermal conductivity detector (TCD) and a 1.1 m carbon molecular sieve of 601 column. The former was used to analyze methane, acetylene, ethane, ethylene and  $\text{C}_3$ – $\text{C}_6$  hydrocarbons, and the latter was used to analyze hydrogen. The reactions investigated are not isometric, so the flow rate of the effluent gas from the reactor was measured by a soapsuds flowmeter.

The parameters investigated in this paper are defined as follows [15]:

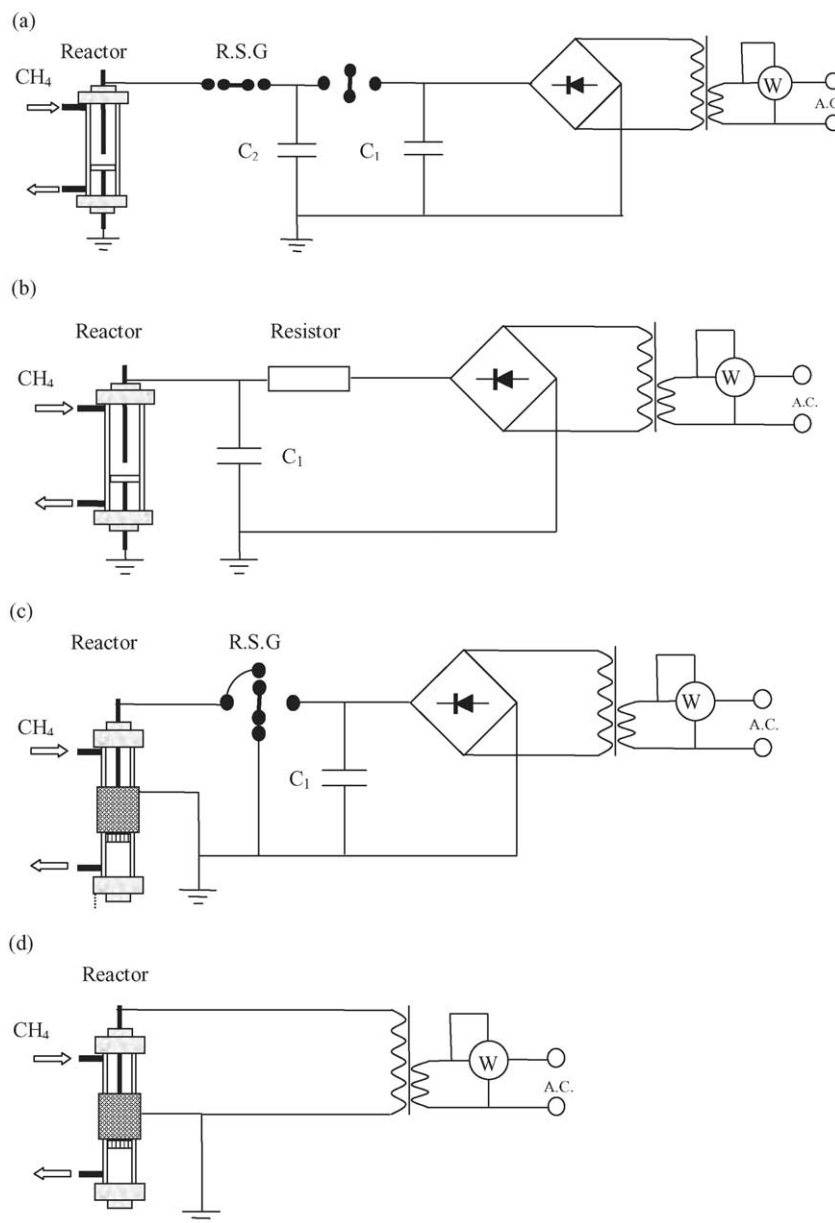


Fig. 1. Schematic diagrams of reactors and circuit layouts: (a) pulsed streamer discharges, (b) pulsed spark discharges, (c) pulsed DC DBD, (d) AC DBD.

(1) Methane conversion ( $X_{\text{CH}_4}$ ) and product yields ( $Y_{\text{C}_x\text{H}_y}$  and  $Y_{\text{H}_2}$ ):

$$X_{\text{CH}_4} (\%) = \frac{\text{moles of CH}_4 \text{ consumed}}{\text{moles of CH}_4 \text{ introduced}} \times 100$$

$$Y_{\text{C}_x\text{H}_y} (\%) = x \left( \frac{\text{moles of C}_x\text{H}_y \text{ produced}}{\text{moles of CH}_4 \text{ introduced}} \right) \times 100$$

$$Y_{\text{H}_2} (\%) = 0.5 \left( \frac{\text{moles of H}_2 \text{ produced}}{\text{moles of CH}_4 \text{ introduced}} \right) \times 100$$

where  $\text{C}_x\text{H}_y$  stands for  $\text{C}_2\text{H}_2$ ,  $\text{C}_2\text{H}_4$ ,  $\text{C}_2\text{H}_6$ , and  $\text{C}_3\text{--C}_6$  hydrocarbons.

(2) Power source efficiency ( $\eta$ , %):

$$\eta = \frac{P_{\text{discharge}}}{P_t} \times 100$$

where  $P_{\text{discharge}}$  is the discharge power and  $P_t$  is the total input power to the power source.

(3) Energy density ( $E_{\text{density}}$ , kJ/mol):

$$E_{\text{density}} = 1344 \frac{P_{\text{discharge}} (W)}{F_{\text{CH}_4} (\text{SCCM})}$$

(4) Energy cost for methane conversion ( $E_{\text{conv}}$ , eV/molecule):

$$E_{\text{conv}} = 13.95 \frac{P_{\text{discharge}} (W)}{F_{\text{CH}_4} (\text{SCCM}) X_{\text{CH}_4}}$$

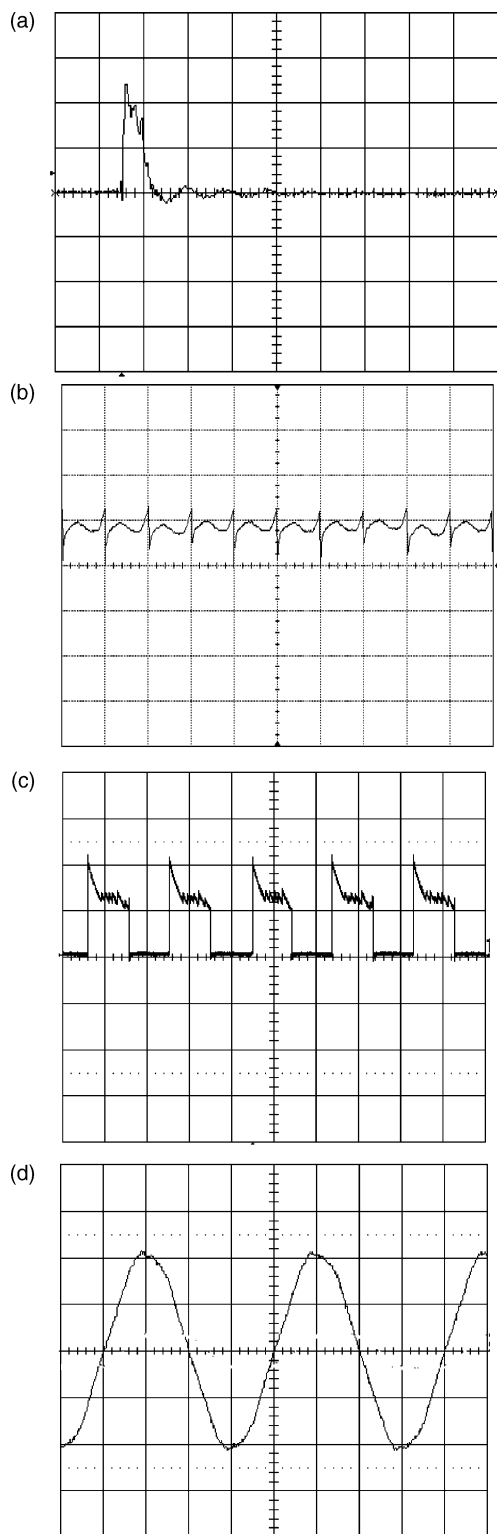


Fig. 2. Voltage waveforms generated from different circuits: (a) pulsed streamer discharges, (b) pulsed spark discharges, (c) pulsed DC DBD, (d) AC DBD. The division of Y-coordinate and X-coordinate: (a) 10 kV and 200 ns, (b) 5 kV and 20 ms, (c) 10 kV and 10 ms, (d) 10 kV and 5 ms.

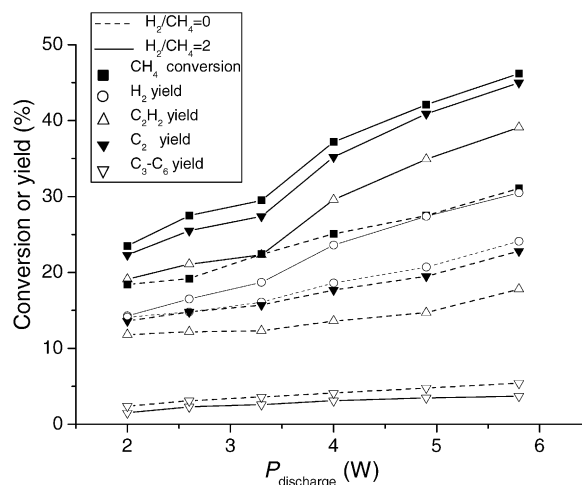


Fig. 3. Methane conversions and product yields in a needle-to-plate reactor by pulsed streamer discharges in pure CH<sub>4</sub> and CH<sub>4</sub> + H<sub>2</sub> (H<sub>2</sub>/CH<sub>4</sub> = 2) systems. Conditions: 55 PPS of pulse frequency, 255 pF of pulse forming capacitor, 15 SCCM of total flow rate.

- (5) Energy cost for product formation ( $E_{C_2H_y}$  and  $E_{H_2}$ , eV/molecule):

$$E_{C_2H_y} = 13.95 \frac{P_{\text{discharge}} (\text{W})}{0.5 F_{CH_4} (\text{SCCM}) Y_{C_2H_y}}$$

$$E_{H_2} = 13.95 \frac{P_{\text{discharge}} (\text{W})}{2 F_{CH_4} (\text{SCCM}) Y_{H_2}}$$

where  $C_2H_y$  is  $C_2H_2$  or  $C_2H_6$ .

### 3. Results and discussion

#### 3.1. Pulsed streamer discharges

The pulsed streamer discharges were driven by using fast-rising narrow pulses of high voltage (12 ns of rise time and about 90 ns of pulse width). Fig. 3 shows the effects of discharge power and H<sub>2</sub> addition on methane conversion, C<sub>2</sub> yield, C<sub>2</sub>H<sub>2</sub> yield and H<sub>2</sub> yield in the plasmas generated by the pulsed streamer discharges. Regardless of the introducing of H<sub>2</sub>, with the increase of discharge power, methane conversion, C<sub>2</sub> yield, C<sub>2</sub>H<sub>2</sub> yield and H<sub>2</sub> yield increase and acetylene is always the dominating product from methane coupling. When hydrogen was added into the feed gas, methane conversion, C<sub>2</sub> yield and C<sub>2</sub>H<sub>2</sub> yield increased remarkably. At 6 W of discharge power, with the addition of hydrogen, methane conversion, C<sub>2</sub> yield and C<sub>2</sub>H<sub>2</sub> yield increased from 31% (pure methane) to 46% (33% methane + 67% hydrogen), 23% (pure methane) to 45% (33% methane + 67% hydrogen), and 18% (pure methane) to 39% (33% methane + 67% hydrogen), respectively. Hydrogen molecules collide with energetic electrons to produce hydrogen radicals and subsequently hydrogen radicals react with other species to form CH<sub>3</sub>, CH<sub>2</sub>, and CH radicals, from which C<sub>2</sub> hydrocarbon products are

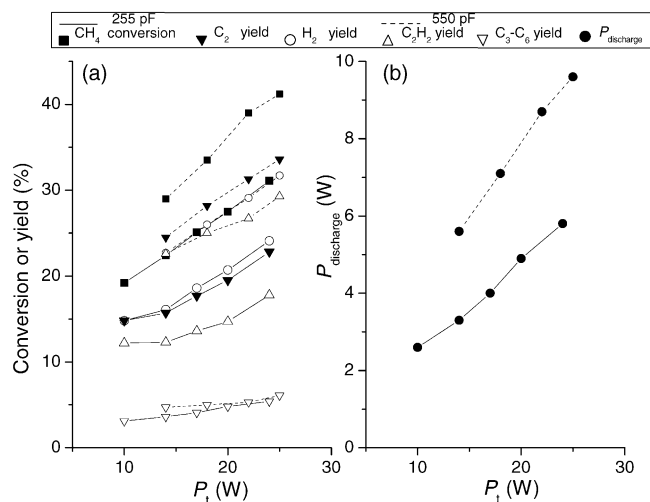


Fig. 4. Effect of pulse forming capacitor on methane conversions and product yields in a needle-to-plate reactor by pulsed streamer discharges. Conditions: 55 PPS of pulse frequency, 15 SCCM of total flow rate, pure methane.

formed. Kirikov et al. used numerical simulation to investigate the kinetics of reactions in the plasma of spark discharges and their results show that  $\text{CH}_2$  radicals in discharge channel react very rapidly with hydrogen radicals to form  $\text{CH}$  radicals, which leads to the increase in the formation of acetylene [16]. Additionally, from Fig. 3, it can easily be seen that  $\text{H}_2$  yield is higher than  $\text{C}_2\text{H}_2$  yield in pure  $\text{CH}_4$  case but lower than  $\text{C}_2\text{H}_2$  yield in  $\text{CH}_4 + \text{H}_2$  case. This result implies that  $\text{H}_2$  addition does restrain the deposition of carbon.

Fig. 4 reveals the effect of pulse forming capacitor on methane conversion,  $\text{C}_2$  yield,  $\text{C}_2\text{H}_2$  yield and  $\text{H}_2$  yield. The results show that 550 pF of pulse forming capacitor gives higher methane conversion,  $\text{C}_2$  yield,  $\text{C}_2\text{H}_2$  yield and  $\text{H}_2$  yield than 255 pF of pulse forming capacitor. It can be seen that, although at the same total input power, 550 pF of pulse forming capacitor releases more energy into the reactor than 255 pF of pulse forming capacitor, which leads to the increase of power source efficiency from about 25% (255 pF case) to about 40% (550 pF case).

### 3.2. Pulsed spark discharges

The pulsed spark discharges examined here were carried out in the same reactor which was mentioned above. But, unlike the above-mentioned fast-rising narrow pulse which was generated by rotary spark gap, the pulses of high voltage were generated by a circuit consisting of a resistor and a capacitor as shown in Fig. 1(b). Methane conversion was examined. Similar to what has taken place in pulsed streamer discharges, acetylene is also the dominating product in pulsed spark discharges. Fig. 5 shows the curves of methane conversion,  $\text{C}_2$  yield and hydrogen yield versus the discharge power at 37, 15 and 10 SCCM of methane flow rates, respectively. From Fig. 5, it can be easily seen that methane

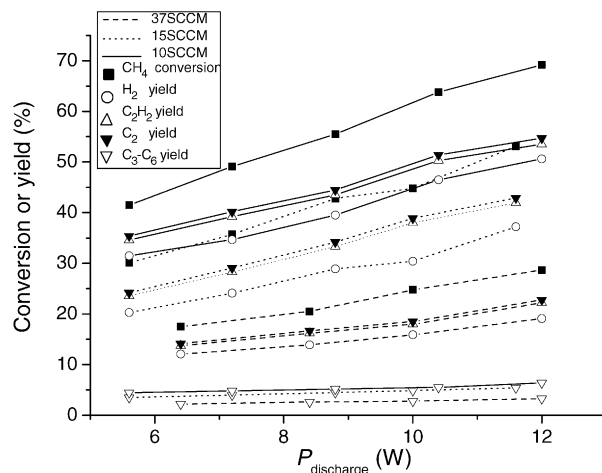


Fig. 5. Methane conversions and product yields in a needle-to-plate reactor by pulsed spark discharges in pure methane.

conversion,  $\text{C}_2$  yield and hydrogen yield increase with the discharge power and decrease with methane flow rate. In addition, at 37 SCCM of methane flow rate and 12 W of discharge power, methane conversion, acetylene yield,  $\text{C}_2$  yield and  $\text{H}_2$  yield were 29, 22, 23 and 19%, respectively; at 10 SCCM of methane flow rate and 12 W of discharge power, 69% of methane conversion, 54% of acetylene yield, 55% of  $\text{C}_2$  yield and 51% of  $\text{H}_2$  yield were achieved. Based upon carbon balance, deposited carbon yields at the two above-mentioned conditions were estimated at 3 and 8%, respectively. It is worthwhile to mention that a severe cathode etching was observed after several hours' discharges because of cathode sputtering.

### 3.3. Comparison of electric discharge techniques

Electric discharge techniques can be implemented in many ways, depending upon the electrode configuration and power supply (pulsed, AC or DC). Four different kinds of electric discharge techniques, pulsed streamer discharges, pulsed spark discharges, pulsed DC DBD and AC DBD, were used for methane conversion. Comparison of methane conversion,  $\text{H}_2$  yield,  $\text{C}_2\text{H}_2$  yield,  $\text{C}_2\text{H}_4$  yield and  $\text{C}_2\text{H}_6$  yield in pulsed streamer discharges, pulsed spark discharges, pulsed DC DBD and AC DBD are shown in Fig. 6. Of the four kinds of electric discharge techniques studied, the highest methane conversion,  $\text{C}_2$  yield, acetylene yield and  $\text{H}_2$  yield were obtained in the pulsed spark discharges. Pulsed streamer discharges give methane conversion much like that of pulsed spark discharges, but only at low energy density (less than 500 kJ/mol),  $\text{C}_2\text{H}_2$  yield in pulsed streamer discharges are almost the same as that in pulsed spark discharges. The pulsed DC DBD gives the highest ethane yield. All the four electric discharge techniques give very low ethylene yield (less than 2%) and 2–5% of  $\text{C}_3\text{--C}_6$  hydrocarbons yield. Both of the two DBD techniques give quite low acetylene yield (less than 0.5%).

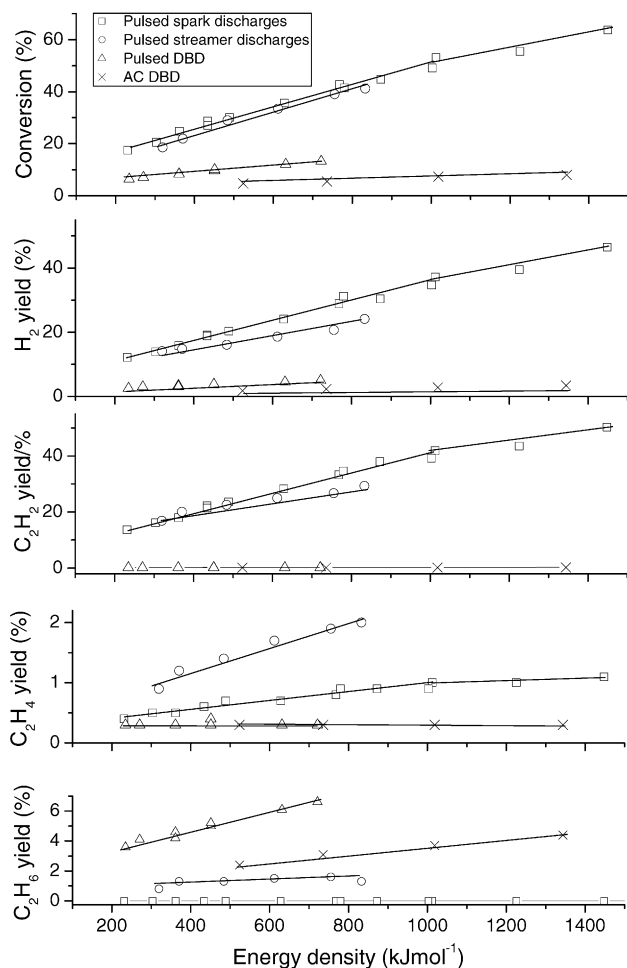
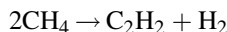
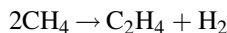
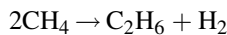


Fig. 6. Comparisons of methane conversions and product yields in the four electric discharge processes in pure methane.

The overall reactions for the formation of ethane, ethylene and acetylene from methane can be expressed as follows:



From thermodynamic calculations, the minimum energy requirement for acetylene formation is 4 eV/molecule and for ethane formation 0.7 eV/molecule, which means that the formation of acetylene requires more energy than that of ethane. In DBD, owing to short-time (<100 ns) and low current pulses (<200 mA), energy per pulse is <0.1 mJ and ethane is the major C<sub>2</sub> products [6].

Fig. 7 points out that energy cost for methane conversion and products formation increases with methane conversion percentage. In pulsed streamer discharges, when methane conversion was increased from 19 to 41%, the increase in energy cost was found to be: from 17 to 21 eV/molecule for methane conversion, from 38 to 59 eV/

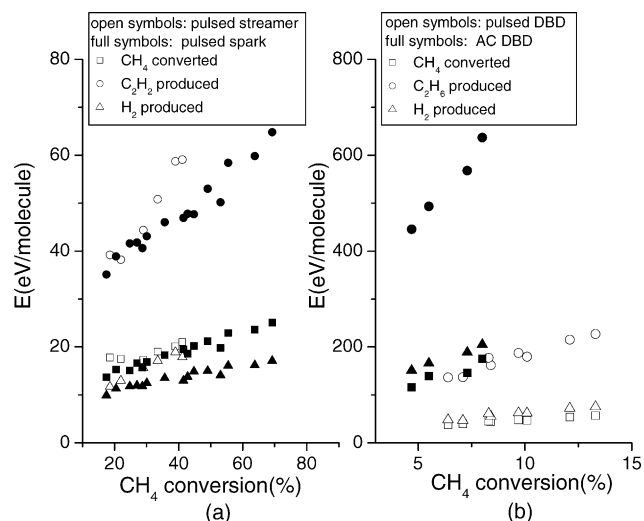


Fig. 7. Energy cost for methane conversion and for C<sub>2</sub>H<sub>2</sub>, C<sub>2</sub>H<sub>6</sub> and H<sub>2</sub> formation as a function of methane conversion percentage.

molecule for acetylene formation and from 12 to 19 eV/molecule for H<sub>2</sub> formation. In pulsed spark discharges, when methane conversion was increased from 18 to 69%, the increase in energy cost was found to be: from 14 to 25 eV/molecule for methane conversion, from 35 to 65 eV/molecule for acetylene formation and from 10 to 17 eV/molecule for H<sub>2</sub> formation. It has been reported [17] that, in a needle-to-needle reactor, pulsed spark discharges required the lowest energy cost for acetylene formation (12 eV/molecule) at 10% methane conversion. However, when the methane conversion reached over 65%, the energy cost for acetylene formation rapidly increased to ca. four times.

In DBD, as mentioned above, ethane was the main hydrocarbon product from methane conversion, consequently, energy cost for ethane formation was investigated instead of that for acetylene formation in pulsed spark discharges and pulsed streamer discharges. For pulsed DBD, with methane conversion of 6–13%, energy cost is in the range of 38–57 eV/molecule for methane conversion, 137–227 eV/molecule for ethane formation, and 47–75 eV/molecule for H<sub>2</sub> formation, respectively. For AC DBD, with methane conversion of 5–8%, energy cost is in the range of 116–175 eV/molecule for methane conversion, 446–637 eV/molecule for ethane formation and 151–205 eV/molecule for H<sub>2</sub> formation, respectively. Undoubtedly, it may be concluded that, of the four kinds of electric discharge techniques studied, pulsed spark discharges require the lowest energy cost for methane conversion and acetylene and hydrogen formation.

#### 3.4. Methane conversion under plasmas over $\gamma\text{-Al}_2\text{O}_3$ pellets

In order to convert methane to the desired products (such as ethylene, benzene) with high selectivity and improve



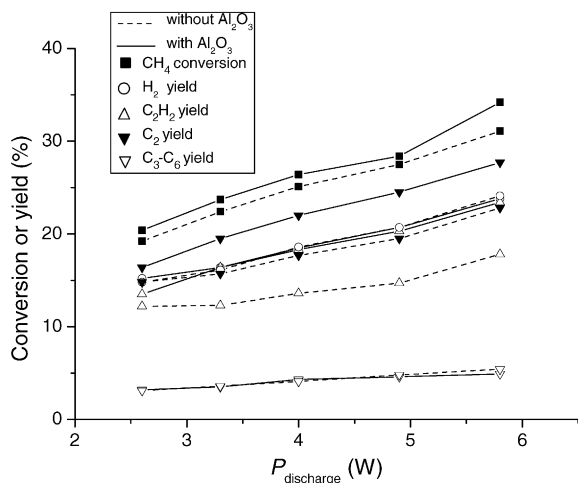


Fig. 8. Effect of immersion of  $\gamma$ - $\text{Al}_2\text{O}_3$  in the pulsed streamer discharges on methane conversions and product yields. Conditions: 55 PPS of pulse frequency, 255 pF of pulse forming capacitor, pure methane, 15 SCCM of flow rate.

energy efficiency, the combination of plasma with catalyst has been explored actively [18–21]. The one-stage plasma-over-catalyst (POC) system, where the catalyst pellets are immersed in the discharge plasmas, was commonly used as plasma and catalyst combined system for methane conversion. It should be mentioned that, in the one-stage POC system, the use of pellet packed in the discharge plasmas does cause change on discharge itself, even though the packed material is not a catalyst. In DBD, it was found that the methane conversion rate increased in the presence of dielectric granular packing (quartz glass and silica gel) [22]. In our experiments,  $\gamma$ - $\text{Al}_2\text{O}_3$  pellets (1–1.5 mm in diameter) were immersed in pulsed streamer discharges, pulsed spark discharges, pulsed DC DBD and AC DBD, and investigated, respectively. It was found that, for the pulsed spark discharges, some carbonaceous threads were easily formed between the needle electrode and the  $\gamma$ - $\text{Al}_2\text{O}_3$ , which was

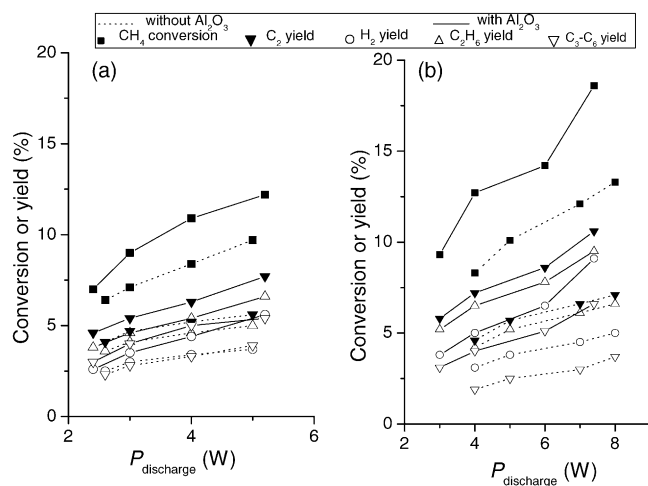


Fig. 9. Effect of immersion of  $\gamma$ - $\text{Al}_2\text{O}_3$  in the pulsed DC DBD on methane conversions and product yields. Conditions: pure methane, 15 SCCM of flow rate, 55 PPS (a) or 110 PPS (b) of pulse frequency.

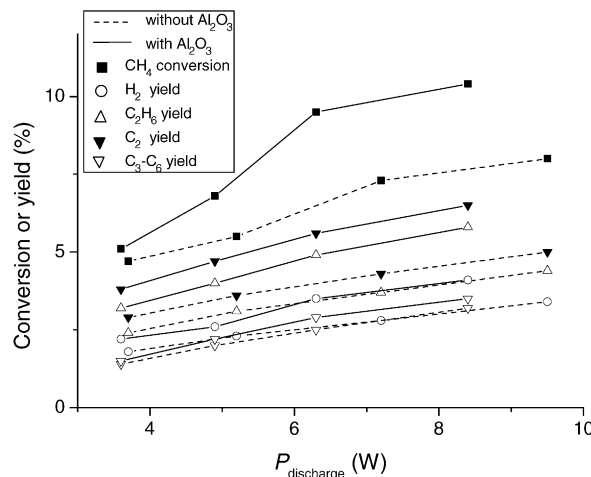


Fig. 10. Effect of immersion of  $\gamma$ - $\text{Al}_2\text{O}_3$  in the AC DBD on methane conversions and product yields. Conditions: pure methane, 10 SCCM of flow rate, 50 Hz of frequency.

placed on the plate electrode. The discharge became very unstable. Figs. 8–10 show the effects of  $\gamma$ - $\text{Al}_2\text{O}_3$  immersed in the discharge plasmas on methane conversion,  $\text{C}_2$  yield and  $\text{H}_2$  yield in pulsed streamer discharges, pulsed DC DBD and AC DBD, respectively. For the above three discharge processes, one can easily draw a conclusion that the immersion of the  $\gamma$ - $\text{Al}_2\text{O}_3$  pellets in the discharge plasmas exhibits a positive effect on increasing methane conversion and  $\text{C}_2$  yield. Gadzhieva [23] used diffuse scattering IR spectroscopy to study methane adsorption and plasma-assisted catalytic conversion on the surface of  $\gamma$ - $\text{Al}_2\text{O}_3$ . It was found that  $\text{CH}_4$  adsorption sites on the  $\gamma$ - $\text{Al}_2\text{O}_3$  surface were formed by molecular and dissociative mechanisms under the action of an electric discharge plasma at room temperature, which leads to the formation of acetylene and other hydrocarbons.

From Fig. 8, one can easily also see that, immersing  $\gamma$ - $\text{Al}_2\text{O}_3$  in the pulsed streamer discharge plasmas causes no obvious change in  $\text{H}_2$  yield even though methane conversion and  $\text{C}_2$  yield clearly increase. This may be interpreted as follows: the immersion of  $\gamma$ - $\text{Al}_2\text{O}_3$  in the pulsed streamer discharge plasmas, on one hand, leads to the increase of methane conversion, which is in favor of  $\text{H}_2$  production. On the other hand, the immersion of  $\gamma$ - $\text{Al}_2\text{O}_3$  can also lower the selectivity to deposited carbon (for example, at  $P_{\text{discharge}} = 3.3$  W, based upon carbon balance, the selectivities to deposited carbon with and without the immersion of  $\gamma$ - $\text{Al}_2\text{O}_3$  were estimated at 3 and 14%, respectively), thus cause the decrease of  $\text{H}_2$  selectivity. Consequently, the contradictory effects of the two above-mentioned facts lead to the result of  $\text{H}_2$  yield in Fig. 8. Moreover, in Figs. 9 and 10, since methane conversion is low and ethane is the main  $\text{C}_2$  products, the deposition of carbon is less significant, which makes  $\text{H}_2$  yield increase along with the increase of methane conversion and  $\text{C}_2$  yield.

#### 4. Conclusions

In the non-thermal plasmas generated by the four different electric discharge techniques, pulsed streamer discharges, pulsed spark discharges, pulsed DC DBD and AC DBD, methane conversion to C<sub>2</sub> hydrocarbons and hydrogen has been studied at atmospheric pressure and ambient temperature. In the former two electric discharge processes, acetylene is the dominating C<sub>2</sub> product. The highest acetylene yield (54%) and H<sub>2</sub> yield (51%) with 69% of methane conversion were obtained, using a needle-to-plate reactor by pulsed spark discharges, in a pure methane system and at 10 SCCM of flow rate and 12 W of discharge power. In the two DBD processes, ethane is the major C<sub>2</sub> products and the pulsed DC DBD process provides the highest ethane yield. In the four electric discharge processes, ethylene yield is less than 2%. Energy costs for methane conversion, acetylene or ethane (for DBD processes) formation, and H<sub>2</sub> formation increase with methane conversion percentage, and were found to be: in pulsed spark discharges (methane conversion 18–69%), 14–25, 35–65 and 10–17 eV/molecule; in pulsed streamer discharges (methane conversion 19–41%), 17–21, 38–59, and 12–19 eV/molecule; in pulsed DBD (methane conversion 6–13%), 38–57, 137–227 and 47–75 eV/molecule; in AC DBD (methane conversion 5–8%), 116–175, 446–637, and 151–205 eV/molecule, respectively.

The immersion of the  $\gamma$ -Al<sub>2</sub>O<sub>3</sub> pellets in the pulsed streamer discharges, or the pulsed DC DBD, or the AC DBD exhibits a positive effect on increasing methane conversion and C<sub>2</sub> yield.

#### Acknowledgements

The present work is supported by National Natural Science Foundation of China (Grant No. 20106003), Fok Ying Tung Education Foundation (Grant No. 94015) and the Provincial Grants of Science and Technology of Liaoning, China (No. 20032126).

#### References

- [1] C.-J. Liu, R. Mallinson, L. Lobban, *J. Catal.* 179 (1998) 326–334.
- [2] S. Kado, Y. Sekine, K. Fujimoto, *Chem. Commun.* (1999) 2485–2486.
- [3] A.-M. Zhu, W.-M. Gong, X.-L. Zhang, B.-A. Zhang, *Sci. China (Ser. B)* 43 (2000) 208–214.
- [4] S.-L. Yao, E. Suzuki, N. Meng, A. Nakayama, *Energy Fuels* 15 (2001) 1300–1303.
- [5] S.-L. Yao, E. Suzuki, N. Meng, A. Nakayama, *Plasma Chem. Plasma Process.* 22 (2002) 225–237.
- [6] Y. Yang, *Ind. Eng. Chem. Res.* 41 (2002) 5918–5926.
- [7] S. Kado, Y. Sekine, T. Nozaki, K. Okazaki, *Catal. Today* 89 (2004) 47–55.
- [8] K. Thanyachotpaiboon, S. Chavadej, T.A. Caldwell, L.L. Lobban, R.G. Mallinson, *AIChE J.* 44 (1998) 2252–2257.
- [9] B. Eliasson, C.-J. Liu, U. Kogelschatz, *Ind. Eng. Chem. Res.* 39 (2000) 1221–1227.
- [10] H.-K. Jeong, S.-C. Kim, C. Han, H. Lee, H.-K. Song, B.-K. Na, *Kor. J. Chem. Eng.* 18 (2001) 196–201.
- [11] A.-M. Zhu, X.-L. Zhang, X.-S. Li, W.-M. Gong, *Sci. China (Ser. B)* 45 (2002) 426–434.
- [12] S.-L. Yao, A. Nakayama, E. Suzuki, *Catal. Today* 71 (2001) 219–223.
- [13] A. Mizuno, K. Shimizu, A. Chakrabarti, L. Dascalescu, S. Furuta, *IEEE Trans. Ind. Appl.* 31 (1995) 957–963.
- [14] K. Ohe, K. Kamiya, T. Kimura, *IEEE Trans. Plasma Sci.* 27 (1999) 1582–1587.
- [15] M. Heintze, M. Magureanu, *J. Appl. Phys.* 92 (2002) 2276–2283.
- [16] A.V. Kirikov, V.V. Ryzhov, A.I. Suslov, *Tech. Phys. Lett.* 25 (1999) 794–795.
- [17] S. Kado, Y. Sekine, T. Nozaki, K. Okazaki, *Catal. Today* 89 (2004) 47–55.
- [18] B. Pietruszka, K. Anklam, M. Heintze, in: *Proceedings of the 16th International Symposium on Plasma Chemistry (ISPC-16)*, Taormina, Italy, June, 2003, p. 582.
- [19] T. Hammer, T. Kappes, W. Schiene, in: C.-J. Liu, R.G. Mallinson, M. Aresta (Eds.), *Utilization of Greenhouse Gases*, ACS Symposium Series No. 852, Section 6, No. 19, 2002.
- [20] T. Nozaki, N. Muto, S. Kado, K. Okazaki, *Catal. Today* 89 (2004) 57–65.
- [21] A.-M. Zhu, X.-L. Zhang, W.-M. Gong, B.-A. Zhang, *Plasma Sci. Technol.* 1 (1999) 61–66.
- [22] K. Schmidt-Szalowski, T. Opalinska, J. Sentek, K. Krawczyk, J. Rusznik, T. Zielinski, K. Radomska, *J. Adv. Oxid. Technol.* 7 (2004) 39–50.
- [23] N.N. Gadzhieva, *High Energy Chem.* 37 (2003) 38–43.